International Journal of Thermal Sciences 49 (2010) 256–263

Contents lists available at ScienceDirect

International Journal of Thermal Sciences

journal homepage: www.elsevier.com/locate/ijts

Internal flows which transist from turbulent through intermittent to laminar

J.P. Abraham [a,*], E.M. Sparrow [b], J.C.K. Tong [b], D.W. Bettenhausen [b]

[a] Laboratory for Heat Transfer and Fluid Flow Practice, School of Engineering, University of St. Thomas, St. Paul, MN 55105-1079, USA
[b] Laboratory for Heat Transfer and Fluid Flow Practice, Department of Mechanical Engineering, University of Minnesota, Minneapolis, MN 55455-0111, USA

ARTICLE INFO

Article history:
Received 16 March 2009
Received in revised form
14 July 2009
Accepted 14 July 2009
Available online 3 August 2009

Keywords:
Flow transition
Laminarization
Intermittent flow
Laminar
Turbulent
Flow regime

ABSTRACT

A transition model for internal flows which enables the prediction of the change of flow regime from turbulent through intermittent to laminar has been implemented by numerical simulation. This model had previously been demonstrated to be effective for the prediction of the breakdown of an initially laminar internal flow and its subsequent transitions to either intermittent or turbulent states. The model was employed here to study a flow which is decelerated by passing through a conical diffuser. The flow enters the diffuser with a fully developed turbulent velocity profile and exhibits transitions either in the diffuser or in a pipe situated downstream of the diffuser exit. The presence or absence of flow separation affected the onset of laminarization. Proof that laminarization actually occurred is provided by the values of the fully developed friction factors in the pipe downstream of the exit of the diffuser. These friction factors spanned the range from pure laminar flow through intermittent flow to fully turbulent flow. Comparisons were made with established benchmarks for each of these three flow regimes.

1. Introduction

Laminarization of initially turbulent flows can be brought about by a variety of mechanisms. A pair of papers by Sreenivasan and Narasihma [1,2] describes various modalities of laminarization. The most frequently studied modality of laminarization is rapid acceleration. A representative collection of papers in this area includes Launder [3], Moretti and Kays [4], Patel and Head [5], Bradshaw [6], Narayanan and Ramjee [7], Greenblatt et al., [8,9], He and Jackson [10], and Kays et al., [11]. This mode creates locally laminar flows in wall-adjacent regions.

Another common mechanism is the heating of a turbulently flowing gas. Since the viscosity of a gas increases with increasing temperature, the heating gives rise to a diminution of the Reynolds number [12,13]. The cooling of liquids can also lead to laminarization since, for liquids, the viscosity increases as the temperature decreases.

In addition to the foregoing laminarization mechanisms, another modality is deceleration of the bulk flow. Various situations in this category include enlarging cross sections of tubes and channels [14,15], bifurcations [16], and radial outflows. In all these cases, the bulk velocity of the flowing fluid diminishes in the direction of flow with a concomitant decrease of the Reynolds number.

In the present investigation, a fully predictive model is set forth for the transition of an initially turbulent internal flow into either intermittent or laminar flow in situations where the flow cross section increases in the streamwise direction. The specific case to be considered is a pipe which delivers a fully developed turbulent flow to the inlet of a conical diffuser. From the diffuser exit, the flow passes smoothly into a circular pipe in which further development occurs. The downstream pipe is sufficiently long to enable the establishment of either fully developed laminar or intermittent flow. The model used here is able to predict the flow regime without user interaction or instruction. The parameter range of the work was extended to cases where both the upstream and downstream flows are turbulent. Special attention is given to the nature of the region of separated flow which is formed in the conical diverging section and its possible extension into the downstream straight pipe.

2. Physical and mathematical models

2.1. Physical model

A schematic diagram of the physical situation to be investigated here is shown in Fig. 1. As seen there, a pipe of circular cross section and diameter d delivers a fully developed turbulent flow to the inlet of a conical diffuser. The diffuser is defined by the total angle of

* Corresponding author. Tel.: +1 651 962 5766; fax: +1 651 962 6419.
E-mail address: jpabraham@stthomas.edu (J.P. Abraham).

1290-0729/$ – see front matter © 2009 Elsevier Masson SAS. All rights reserved.
doi:10.1016/j.ijthermalsci.2009.07.013

Nomenclature

a	SST model constant
c	constants used in the intermittency transport equation
d	upstream diameter
D	downstream diameter
E	model destruction terms
f	fully developed friction factor
F_1, F_2	blending functions in SST model
F_{Length}	empirical-based correlation which controls the length of the transition region
k	turbulent kinetic energy
$\dot{m}$	mass flow rate
p	pressure
P	model production term
r	radial coordinate
Re	Reynolds number, $4\dot{m}/\mu\pi d$ or $4\dot{m}/\mu\pi D$
S	absolute value of the shear strain rate
u	velocity
x	streamwise coordinate
x_i	tensor coordinate

Symbols

α	SST model constant
β_1, β_2	SST model constants
ω	specific rate of turbulence dissipation
μ	dynamic viscosity
θ	total angle of divergence
$\pounds$	laminarization parameter
Π	intermittency adjunct function
γ	intermittency
ρ	density
σ	Prandtl-number-like diffusion parameters
τ	shear stress
Ω	magnitude of the vorticity

Subscripts

i, j	tensor indices
t	turbulent

expansion θ and the ratio D/d of the outlet to inlet diameters of the diffuser. The flow leaving the diffuser is discharged into a pipe of larger diameter D having a streamwise length sufficiently long to enable fully developed flow to be attained.

The numerical simulations will be performed for three values of the diffuser angle θ: 5, 10, and 30°. For each of these diffuser angles, the diameter ratio D/d was assigned values of 2, 3, and 4. The Reynolds number at the inlet of the diffuser ranged from 4000 to approximately 50,000.

2.2. Governing equations

The mathematical model on which the laminarization analysis is based is an evolution of that due to Menter et al. [17–19] which was concerned with laminar-to-turbulent transition for an *external boundary layer* flow. Very recently, the Menter model was compared with two other external-flow transition models by Suluksna and Juntasaro [20], who found that it provides the closest representation of experimental data for a number of test cases. This model was further developed by the present authors [21] to extend its applicability to *internal flows*. In particular, in that paper, the focus of the work was on the transition of initially laminar flows to either intermittent or turbulent flows in straight, round pipes. The outcome of that investigation demonstrated the validity of the model for internal flows. Subsequently, the authors extended the model to planar internal flows to demonstrate the breadth of its capability of dealing with laminar flows and their subsequent transitions [22]. The success of the extended model has motivated this investigation which deals with the inverse evolution of flow regimes relative to those that have been studied previously. As has already been mentioned, the present focus is on initially turbulent flows and their evolution into other regimes.

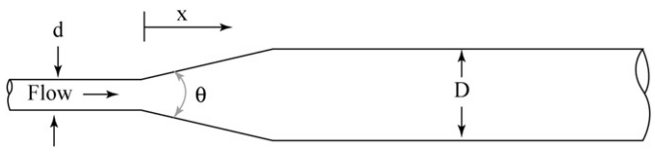

Fig. 1. Schematic diagram of the physical situation. The flow enters the diffuser with a fully developed turbulent velocity profile.

The mathematical model encompasses three sets of interlocking equations. The first set of governing equations is the well-known continuity and RANS equations, which are

$$\frac{\partial u_i}{\partial x_i} = 0 \tag{1}$$

$$\rho\left(u_i\frac{\partial u_j}{\partial x_i}\right) = -\frac{\partial p}{\partial x_j} + \frac{\partial}{\partial x_i}\left((\mu+\mu_t)\frac{\partial u_j}{\partial x_i}\right) \quad j = 1,2,3 \tag{2}$$

In these equations, μ_t is the so-called turbulent viscosity. To obtain values of this quantity, it is necessary to make use of a supplementary pair of equations. In the present instance, since the transitional model is linked to the shear-stress transport model of turbulence (SST), the latter must be used for the determination of μ_t [23]. The dependent variables of the SST model are the turbulence kinetic energy k and the specific rate of turbulence destruction ω. The governing equations for these quantities are

$$\frac{\partial(\rho u_i k)}{\partial x_i} = \gamma P_k - \beta_1\rho k\omega + \frac{\partial}{\partial x_i}\left[\left(\mu+\frac{\mu_t}{\sigma_k}\right)\frac{\partial k}{\partial x_i}\right] \tag{3}$$

and

$$\frac{\partial(\rho u_i \omega)}{\partial x_i} = \alpha\rho S^2 - \beta_2\rho\omega^2 + \frac{\partial}{\partial x_i}\left[\left(\mu+\frac{\mu_t}{\sigma_{\omega 1}}\right)\frac{\partial\omega}{\partial x_i}\right] + 2(1-F_1)\rho\frac{1}{\sigma_{\omega 2}\omega}\frac{\partial k}{\partial x_i}\frac{\partial\omega}{\partial x_i} \tag{4}$$

The solution of Eqs. (3) and (4) yields the turbulent viscosity μ_t in terms of k and ω. This relationship is

$$\mu_t = \frac{a\rho k}{\max(a\omega, SF_2)} \tag{5}$$

in which F_2 is a blending function that limits the eddy viscosity within the boundary layer. Equation (3) is, in actuality, a modification of the original version of the SST model in that it contains a multiplying factor γ, termed the intermittency, which acts on the turbulence production term P_k. In the conventional form of the SST

model, the factor 1 appears in lieu of γ. It is the role of γ to diminish the turbulence production term in regions of turbulence intermittency or laminar flow. Further details of the SST model can be found in [23].

The equation used for the prediction of γ is [17–19]

$$\frac{\partial(\rho u_i \gamma)}{\partial x_i} = P_{\gamma,1} - E_{\gamma,1} + P_{\gamma,2} - E_{\gamma,2} + \frac{\partial}{\partial x_i}\left[\left(\mu + \frac{\mu_t}{\sigma_\gamma}\right)\frac{\partial \gamma}{\partial x_i}\right] \tag{6}$$

Equation (6) contains two production terms ($P_{\gamma,1}$ and $P_{\gamma,2}$) and two destruction terms ($E_{\gamma,1}$ and $E_{\gamma,2}$) which are defined by:

$$\begin{aligned} P_{\gamma,1} &= 2F_{\text{length}}\rho S(\gamma F_{\text{onset}})^{c_{\gamma 3}} \\ P_{\gamma,2} &= 2c_{\gamma 1}\rho\Omega\gamma F_{\text{turb}} \\ E_{\gamma,1} &= \gamma P_{\gamma,1} \\ E_{\gamma,2} &= c_{\gamma 2}\gamma P_{\gamma,2} \end{aligned} \tag{7}$$

where S is the magnitude of the strain rate, F_{length} is an empirical correlation which controls the length of the transition zone, and Ω is the magnitude of the vorticity [17–19]. The original values of the constants specified by Menter are

$$\begin{aligned} c_{\gamma 1} &= 0.03 \\ c_{\gamma 2} &= 50 \\ c_{\gamma 3} &= 0.5 \end{aligned} \tag{8}$$

These values were chosen by Menter on the basis of experimental data for external flows. To enable the model to be applicable to internal flows, it was necessary to change

$$c_{\gamma 2} = 0.015, c_{\gamma 2} = 70 \tag{9}$$

Embedded in the intermittency production and destruction terms, P and E respectively, is the quantity Π which may be designated as the intermittency adjunct function. In the original Menter notation, the intermittency adjunct function was denoted by Re_θ and was termed the transition momentum thickness Reynolds number. Such a designation may appear to describe a quantity resulting from an integration across the boundary layer or cross section. However, Menter intended that Re_θ be a local quantity, dependent on all of the coordinates of the problem. This description did not appear to be sufficiently clear and as a consequence, it was renamed by the present authors. The governing equation for Π is

$$\frac{\partial(\rho u_i \Pi)}{\partial x_i} = P_\Pi + \frac{\partial}{\partial x_i}\left[\sigma_\Pi(\mu + \mu_t)\frac{\partial \Pi}{\partial x_i}\right] \tag{10}$$

The mathematical statement of the problem is embodied in the eight equations, Eqs. (1)–(4), (6), (10). These equations are strongly coupled and must be solved simultaneously.

2.3. Numerical implementation

The foregoing interrelated set of partial differential equations requires numerical solution, the implementation of which was accomplished by means of ANSYS CFX 11.0 software. In the actual numerical work, extreme care was required in order to obtain accurate solutions. In particular, the density of the mesh in the neighborhood of the pipe walls had to be carefully monitored to obey the condition that the location of the wall-adjacent node satisfy the criterion $y^+ < 1$ ($y^+ = (y\sqrt{\tau/\rho})/\mu$), where y is the perpendicular distance from the wall. The particular issue that had to be addressed in satisfying the y^+ criterion was that the wall shear stress τ varies continuously along all of the solid boundaries. As a consequence, it was necessary to make the y value of the wall-adjacent node sufficiently small so that the foregoing y^+ criterion was obeyed everywhere.

In view of the aforementioned considerations, a large number of nodes had to be used to obtain solutions of acceptable accuracy. To validate mesh independence and accuracy, elements ranging from 215,000 to 430,000 were employed, and comparisons were made between the calculated values of the fully developed friction factor and those from the literature. In all cases, agreement to within 1% or better was achieved. In addition, care was taken to achieve residuals of 10^{-6} or smaller for all variables, except for the residual of the intermittency variable which was typically achieved to within 10^{-5}.

CFX 11.0 software makes use of a false-transient, time-stepping approach to enable convergence to the steady-state solution. While the fully implicit, backward-Euler, time-stepping algorithm exhibits first-order accuracy in time, its use does not affect the accuracy of the final, converged steady-state solution.

Coupling of the velocity–pressure equations was achieved on a non-staggered, collocated grid using the techniques developed by Rhie and Chow [24] and Majumdar [25]. The inclusion of pressure-smoothing terms in the mass conservation equation suppresses oscillations which can occur when both the velocity and pressure are evaluated at coincident locations.

The advection terms in the momentum and energy equations were evaluated by using the upwind values of the momentum flux, supplemented with an advection-correction term. The correction term reduces the occurrence of numerical diffusion (i.e., false diffusion) and is of second-order accuracy. Details of the advection treatment can be found in Barth and Jesperson [26].

In order to achieve a fully developed turbulent flow at the inlet cross section of the diffuser, the solution domain was extended far upstream to provide a sufficient development length. At the upstream end of the extended solution domain, an algebraic representation which closely approximates the fully developed profile was imposed. Also, at that cross section, it was necessary to provide a value of the turbulence intensity Tu, which also enables the determination of the other turbulence quantities (k, ω, and Π). The selected value of Tu was 5%. Furthermore, although the intermittency γ is set equal to 1 at the inlet of the extended solution domain, its value at the diffuser inlet is naturally determined by the model.

At the downstream end of the solution domain, the streamwise second derivatives of all the dependent variables are zero, except for the pressure, for which a specified, area-averaged value is prescribed. At all bounding walls, the no-slip and impermeability conditions are enforced for all the velocity components. Also zero at the wall are the turbulence kinetic energy and the specific dissipation rate as well as the normal derivatives of both γ and Π.

3. Results and discussion

3.1. Mechanism of laminarization

As was suggested by Narashima and Sreenivasan [1], an appropriate parameter which serves as a metric for laminarization is the ratio of turbulence production to turbulence dissipation. However, these authors did not provide any results for this quantity. Here, use is made of the present universal transition model to extract *local* values for the ratio in a variety of different operating conditions. Values of this ratio less than one will be taken to indicate the onset of laminarization. Furthermore, for convenience of discussion, the ratio of production to dissipation will be termed the *laminarization parameter £*.

Evidence of laminarization will be presented in Figs. 2–4. Each of these figures corresponds to a situation in which the Reynolds number at the inlet of the diffuser is 8000, and the diffuser-exit Reynolds number is 2000. These results respectively correspond to diffuser angles θ of 5, 10, and 30° and to a diameter ratio of 4:1.

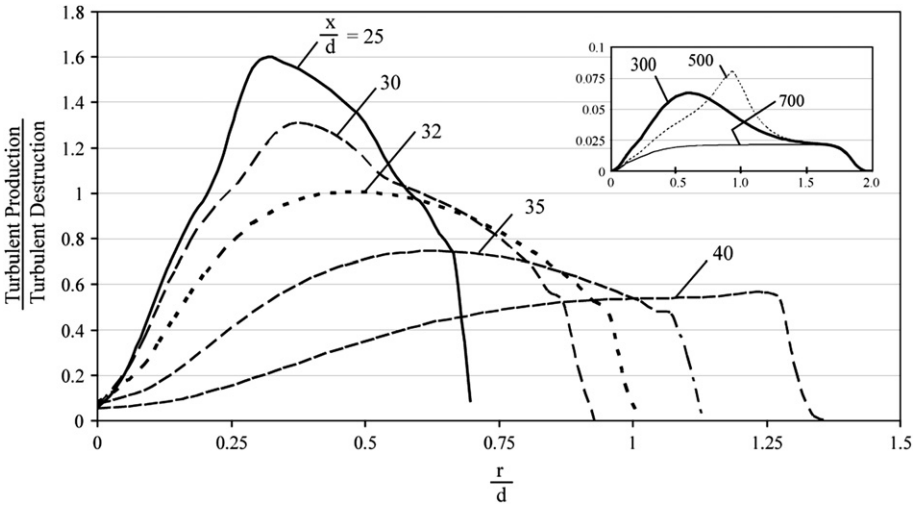

Fig. 2. Radial and axial variations of the laminarization parameter for a diffuser angle of 5°. Diffuser inlet and exit Reynolds numbers of 8000 and 2000, respectively. Diffuser ends at $x/d = 54$.

In each figure, the laminarization parameter £ is plotted as a function of the radial coordinate at each of a number of axial stations along the length of the diffuser. Inspection of the in-diffuser curves (those in the main part of the figure) that are displayed in Fig. 2 indicates that turbulence production is minimal along the axis of the diffuser but increases in the radial outward direction until it reaches a maximum before finally subsiding to zero at the diffuser wall. At successive axial stations, £ decreases and its cross-sectional maximum drops below one. This event occurs at approximately $x/d \sim 32$. Thereafter, further laminarization ensues at increasing downstream distances. Since the diffuser extends to $x/d = 54$, laminarization is initiated in the diffuser.

To demonstrate the continuation of laminarization in the pipe that is downstream of the diffuser exit, an inset has been inserted at the upper right of Fig. 2. It is shown there that the relative rate of production (production related to destruction) does approach very small values at very large values of x/d. However, the decrease of £ to its far downstream value is not monotonic, as evidenced by the successive curves for $x/d = 300$, 500, and 750. This behavior is believed to be due to a local imbalance in the rates of decrease of the production and destruction of turbulence and does not correspond to a rejuvenation of turbulence, as evidenced by the low values of £ and by the friction factor results to be presented shortly.

Similar trends are exhibited in Figs. 3 and 4, but with significant differences in detail. The onset of laminarization occurs at locations closer to the diffuser inlet as the diffuser angle increases. For the 10° case, laminarization also occurs within the diffuser (diffuser extends to $x/d = 37$). However, for the 30° diffuser angle, the onset of laminarization occurs in the pipe downstream of the diffuser (diffuser ends at $x/d = 26$). The shapes of the £ distributions in the diffuser for the 10 and 30° cases reflect the presence of flow separation which was not present for the 5° diffuser. It is believed that the saddle that appears in the distributions for the former cases is due to the separation.

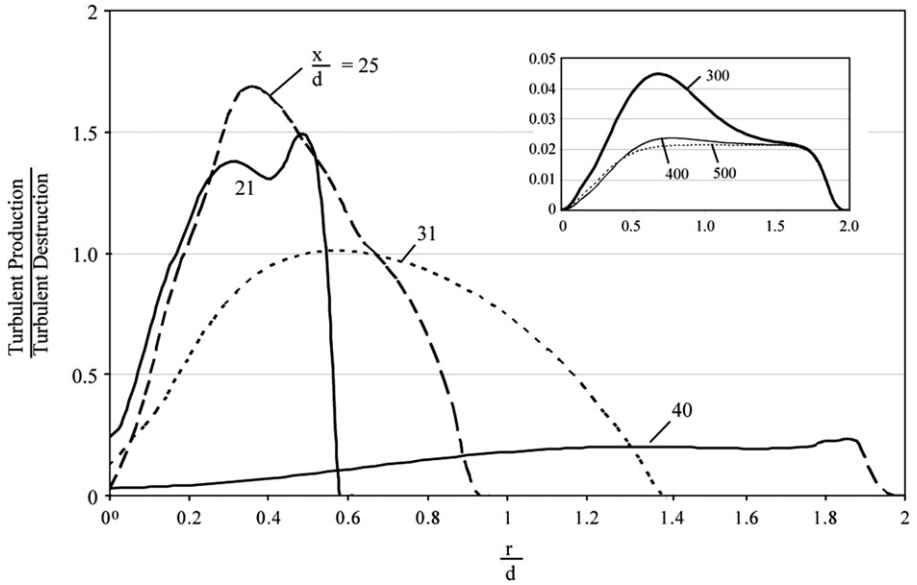

Fig. 3. Radial and axial variations of the laminarization parameter for a diffuser angle of 10°. Diffuser inlet and exit Reynolds numbers of 8000 and 2000, respectively. Diffuser ends at $x/d = 37$.

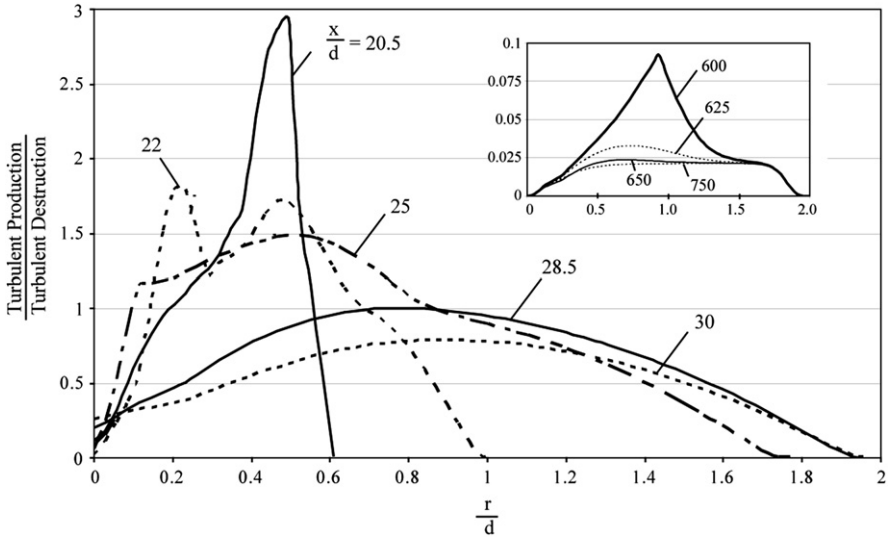

Fig. 4. Radial and axial variations of the laminarization parameter for a diffuser angle of 30°. Diffuser inlet and exit Reynolds numbers of 8000 and 2000, respectively. Diffuser ends at $x/d = 26$.

To elaborate the findings of Figs. 2–4, diffuser-inlet and diffuser-exit Reynolds numbers of 14,400 and 3600 were selected and the results reported in Figs. 5–7 for angles of 5, 10, and 30°, respectively. These cases were chosen to call attention to a situation which yields a *fully developed intermittent* flow regime. This regime was seemingly first identified in [21]. Inspection of the main graphs in Figs. 5–7 shows trends similar to those of the counterpart figures, Figs. 2–4. The unique aspect of Figs. 5–7 is displayed in their insets which show the downstream behavior of the intermittency parameter $\mathcal{E}$. The terminal values of $\mathcal{E}$ are seen to be considerably higher than those displayed in the insets of the preceding set of figures and, in fact, values of $\mathcal{E}$ that are slightly above one are in evidence. Clearly there is turbulence present of a sufficiently high intensity to have a significant impact on the nature of the fluid flow. These observations will be reinforced when fully developed friction factors are displayed.

To illustrate the relationship of the laminarization parameter $\mathcal{E}$ to the Reynolds number in the fully developed intermittent regime, Fig. 8 has been prepared. This figure contains results for two Reynolds numbers, respectively 2770 and 3560, both of which correspond to fully developed intermittency. It is seen in the figure that for both of these Reynolds numbers, $\mathcal{E}$ exceeds one. However, there are interesting differences in detail that are worthy of identification and discussion. First, for the higher of the Reynolds numbers, the peak in the radial distribution of the laminarization parameter occurs closer to the wall than for the lower Reynolds number case. Of greater significance is that the cross-sectional average value of $\mathcal{E}$ is greater for the higher Reynolds number, indicating a closer approach to fully turbulent flow.

3.2. Fully developed friction factors

A compelling demonstration of the capabilities of the laminarization model is provided by the behavior of the fully developed friction factor in the pipe downstream of the diffuser. The friction factor results for all of the cases considered here span three

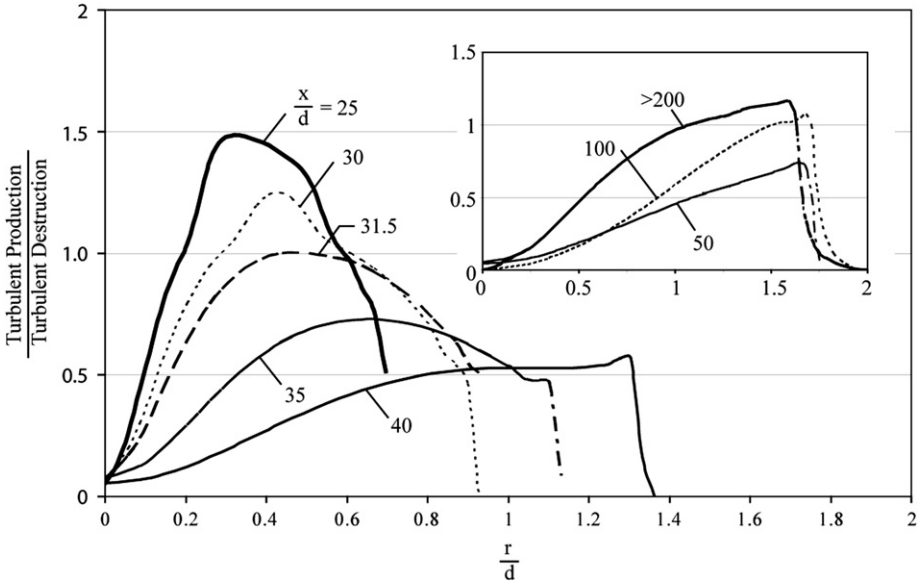

Fig. 5. Radial and axial variations of the laminarization parameter for a diffuser angle of 5°. Diffuser inlet and exit Reynolds numbers of 14,400 and 3600, respectively.

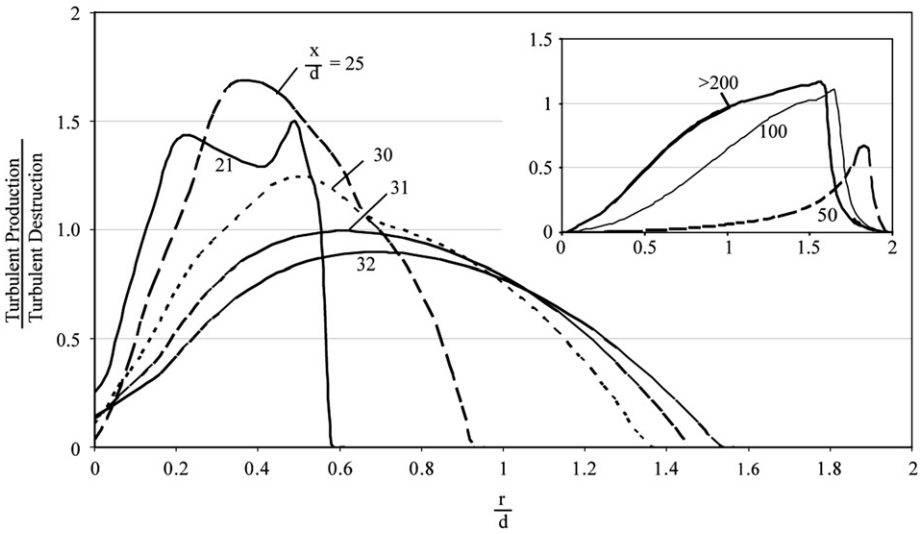

Fig. 6. Radial and axial variations of the laminarization parameter for a diffuser angle of 6°. Diffuser inlet and exit Reynolds numbers of 14,400 and 3600, respectively.

divergence angles and downstream Reynolds numbers ranging from 125 to 12,000. These results are displayed in Fig. 9 where the friction factor is plotted as a function of the downstream Reynolds number. To enable a clear display, the present results are represented by discrete data symbols. It is noteworthy that each "data point" actually represents either two or three individual cases which have the same downstream Reynolds numbers.

In addition to the results of this investigation, a number of benchmarks are included in the figure in order to provide context. These include the laminar friction factor $f = 64/Re$ and the Colebrook [27] representation of the turbulent-flow friction factor which is shown in Eq. (11).

$$f = (1.8 \cdot \log_{10}(Re) - 1.51)^{-2} \tag{11}$$

The figure also contains a curve depicting the friction factor – Reynolds number relationship for flow that undergoes transitions from laminar-to-intermittent-to-turbulent [21].

Inspection of Fig. 9 shows that the results provided by the present universal flow-regime model are in excellent agreement with the laminar and turbulent baseline friction factors and form a logical bridge between these limiting cases. The flow regime which bridges between laminar and turbulent is here termed fully developed intermittent. The figure indicates that there is a slight displacement of the present results from those resulting from transitions from laminar through intermittent to turbulence [21]. The latter is represented by the dotted line in the figure. This slight displacement can be attributed to the fact that the Reynolds number is not necessarily the unique determinant of a flow regime. For example, (Draad, et al., [28]) found that Reynolds numbers as high as 60,000 still corresponded to laminar flow. This outcome was the result of extraordinary precautions to minimize disturbances.

It has already been noted that the present data for the various diffuser angles fall together, indicating that the upstream flow phenomena which occur in the diffuser and in the redevelopment

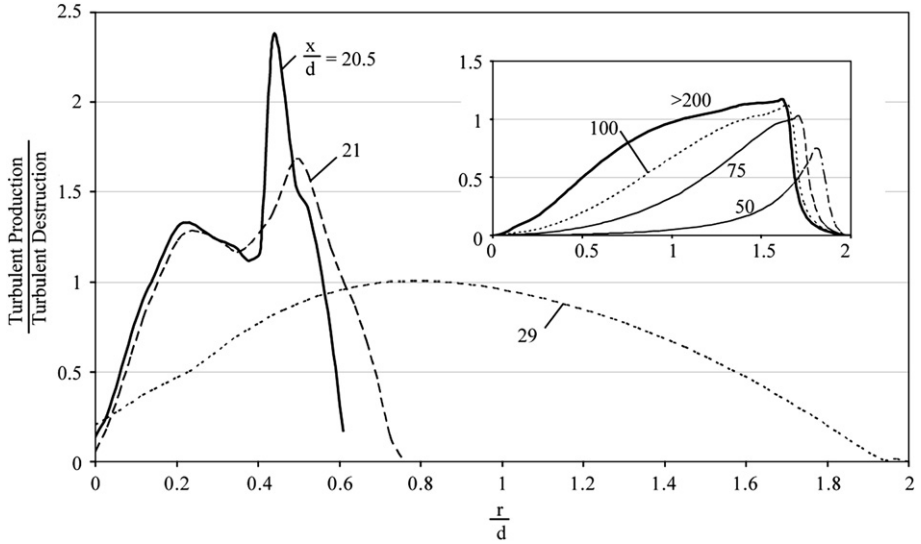

Fig. 7. Radial and axial variations of the laminarization parameter for a diffuser angle of 30°. Diffuser inlet and exit Reynolds numbers of 14,400 and 3600, respectively.

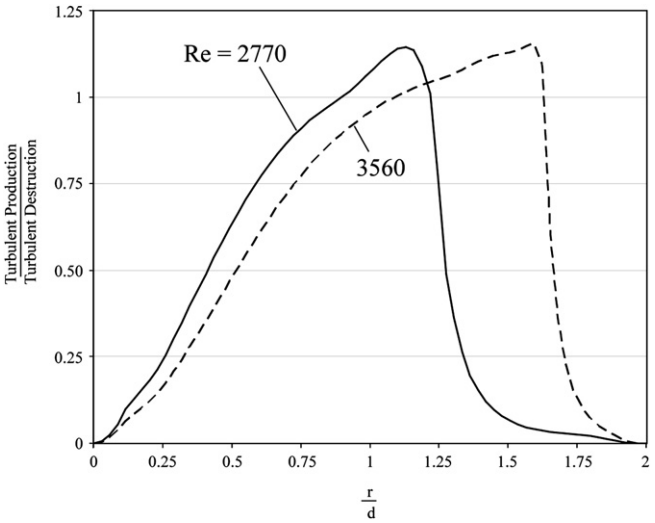

Fig. 8. Comparison of the radial distributions of the fully developed laminarization parameter for downstream Reynolds numbers of 2770 and 3650.

region downstream of the diffuser do not affect the fully developed nature of the flow. The present friction factor results in the fully developed intermittent regime can be represented algebraically as follows

$$f = -3.73 \times 10^{-9} Re^2 + 3.29 \times 10^{-5} Re - 0.0319, \quad 2600 < Re < 4000 \tag{12}$$

In view of the evidence presented in Figs. 2–9, it is believed that the transitional model used here can be regarded as the first demonstration that laminarization can be predicted for internal flows.

4. Concluding remarks

It has been demonstrated here that a flow-regime transition model, originally used for laminar-to-turbulent transitions in internal flows, is also applicable for laminarization in internal flows. The specific situation for which the internal flow model was tested for its laminarization capabilities is the expansion of the flow cross section due to the presence of conical diffusers of various angles. These angles extended over the range from 5 to 30°. For each diffuser, the Reynolds numbers at inlet and exit were varied parametrically to span the entire range of possible transitions. To investigate whether the present model could provide results that would merge smoothly with non-transitional cases, additional Reynolds numbers were chosen outside of the transition range.

To assess the laminarization tendencies, a new metric, termed the *laminarization parameter*, was defined as the ratio of the local rate of turbulence production to the local rate of turbulence destruction. The behavior of this parameter during laminarization was monitored as to when its value decreased below the value of one. This occurrence was judged to be the onset of the laminarization behavior. The onset of laminarization was found to be affected by the presence or absence of flow separation.

Downstream of the onset of laminarization, two possible flow regimes may be attained. For a downstream Reynolds number in the laminar range, the laminarization parameter continues to decrease and reaches values so low that a purely laminar flow sets in. On the other hand, for downstream Reynolds numbers in the fully developed intermittent range, the decline of the value of the laminarization parameter is arrested and a subsequent recovery in its value leads to a terminal presence of moderate turbulence.

A positive proof that laminarization had, in fact, occurred was provided by the values of the fully developed friction factors in the flow far downstream of the exit of the diffuser. These friction factors were in excellent agreement with the well-established laminar and turbulent friction factors and spanned between these regimes. The present results were also compared with those for fully developed intermittent flows obtained in a prior study by the authors for laminar-to-intermittent-to-turbulent transitions. The comparison showed that the patterns of forward and reverse flow transition yielded slightly different values of the friction factor in the regime of intermittency.

On the basis of information presented in this paper, it may be concluded that the flow-regime transition model for internal flows works equally well for flows which transit from laminar through intermittent to turbulent and for flows which transit from turbulent through intermittent to laminar.

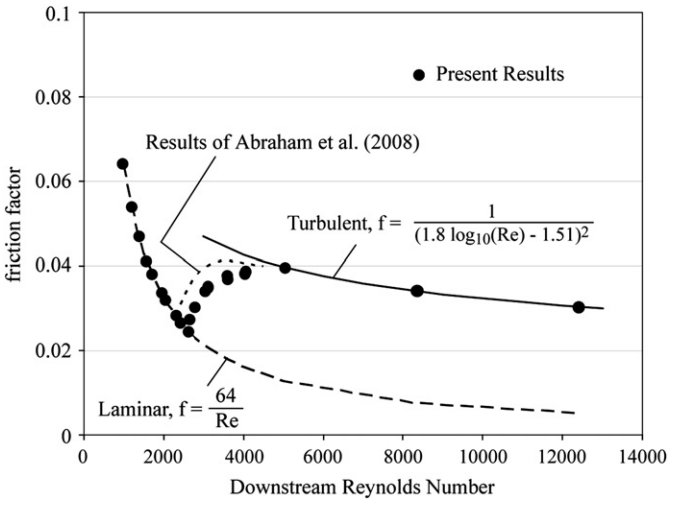

Fig. 9. Variation of the fully developed friction factor with the Reynolds number.

Acknowledgement

Support of H. Birali Runesha and the Supercomputing Institute for Digital Simulation & Advanced Computation at the University of Minnesota is gratefully acknowledged.

References

[1] R. Narashima, K.R. Sreenivasan, Relaminarization of fluid flows, in Advances in Applied Mechanics, Academic Press, Burlington, MA, 1979, pp. 221–309.
[2] K.R. Sreenivasan, Review article: laminarescent, relaminarizing, and retransitional flows, Acta Mech. 44 (1982) 1–48.
[3] B.E. Launder, Laminarization of the turbulent boundary layer by acceleration, Report number 77, Gas Turbine Laboratory, MIT, Cambridge, MA, 1964.
[4] P.M. Moretti, W.M. Kays, Heat transfer to a turbulent boundary layer with varying free-stream velocity and varying surface temperature – an experimental study, Int. J. Heat Mass Transfer 18 (1965) 1187–1202.
[5] V.C. Patel, M.R. Head, Reversion of turbulent to laminar flow, J. Fluid Mech. 34 (part 2) (1968) 371–392.
[6] P. Bradshaw, A note on reverse transition, J. Fluid Mech. 35 (part 2) (1969) 387–390.
[7] M.A. Narayanan, V. Ramjee, On the criteria for reverse transition in a two-dimensional boundary layer flow, J. Fluid Mech. 35 (1969) 225–241.
[8] D. Greenblatt, E.A. Moss, Pipe-flow relaminarization by temporal acceleration, Phys. Fluids 11 (1999) 3478–3481.
[9] D. Greenblatt, E.A. Moss, Rapid temperature accerlation of a turbulent pipe flow, J. Fluid Mech. 514 (2004) 327–350.
[10] S. He, J.D. Jackson, A study of turbulence under conditions of transient flow in a pipe, J. Fluid Mech. 408 (2000) 1–38.

[11] W.M. Kays, M. Crawford, B. Weigand, Convective heat and mass transfer, fourth ed. McGraw-Hill, New York, 2005.
[12] D.M. McEligot, The effect of large temperature gradients on turbulent flow of gases in the downstream region of tubes, PhD Thesis, TID-19446, Standford University, 1963.
[13] C.W. Coon, 1968. The transition from the turbulent to the laminar regime for internal convective flow with large property variations, PhD Thesis, University of Arizona, 1968.
[14] A.H. Gibson, On the flow of water through pipes and passages having converging or diverging boundaries, Proc. R. Soc. London, Series A 83 (1910) 366–378.
[15] M. Sibulkin, Transition from turbulent to laminar pipe flow, Phys. Fluids 5 (1962) 280–284.
[16] P.R. Viswanath, R. Narasimha, A. Prabhu, Visualization of relaminarizing flows, Ind. Instit. Sci. J. Eng. Technol. 60 (1978) 159–165.
[17] F.Menter, T. Esch, S. Kubacki, S., 2002. Transition modeling based on local variables, 5th Int. Symp. on Engineering Turbulence Modeling and Measurements, Mallorca, Spain.
[18] F. Menter, R. Langtry, S. Likki, Y. Suzen, P. Huang, S. Volker, 2004. A correlation –based transition model using local variables, part I – model formulation, in: Proc.. of ASME Turbo Expo Power for Land, Sea, and Air, Vienna, Austria, June 14–17.
[19] F. Menter, R. Langtry, R. Likki, Y. Suzen, P. Huang, S. Volker, 2004. A correlation –based transition model using local variables, part ii – test cases and industrial applications, in: Proc. of ASME Turbo Expo Power for Land, Sea, and Air, Vienna, Austria, June 14–17.
[20] K. Suluksna, E. Juntasaro, Assessment of intermittency transport equations for modeling transition in boundary layers subjected to freestream turbulence, Int. J. Heat Fluid Flow 29 (2008) 48–61.
[21] J. Abraham, J. Tong, E. Sparrow, Numerical simulation of laminar-to-turbulent transition and intermittent internal flows, Num. Heat Tran. A 54 (2008) 103–115.
[22] W. Minkowycz, J. Abraham, E. Sparrow, Numerical simulation of laminar breakdown and subsequent intermittent and turbulent flow in parallel plate channels: effects of inlet velocity profile and turbulence intensity, Int. J. Heat Mass Transfer 52 (2009) 4040–4046.
[23] F. Menter, Two-equation eddy-viscosity turbulence models for engineering applications, AIAA J. 32 (1994) 1598–1605.
[24] C.Rhie, W.Chow, Numerical study of the turbulent flow past an isolated airfoil with trailing edge separation, AIAA paper no. 82-0998, 1982.
[25] S. Majumdar, Role of underrelaxation in momentum interpolation for calculation of flow with nonstaggered grids, Numer. Heat Transfer 13 (1988) 125–132.
[26] T.Barth, D.Jesperson, The design and applications of upwind schemes on unstructured meshes, AIAA paper no. 89-03, 1989.
[27] C. Colebrook, Turbulent flow in pipes with particular reference to the transition between smooth and rough pipe laws, J. Inst. Civ. Eng. London 11 (1938) 133–156.
[28] A. Draad, G. Kuiken, F. Nieuwstady, Laminar-turbulent transition in pipe flow for Newtonian and non-Newtonian fluids, J. Fluid Mech. 377 (1998) 267–312.